engineering proceedings

Proceeding Paper

An Optimization Approach for Demand-Side Scheduling in Microgrid Energy Management System †

Kayode Ebenezer Ojo [1], Akshay Kumar Saha [1,*] and Viranjay M. Srivastava [1,2]

[1] Discipline of Electrical, Electronic and Computer Engineering, University of KwaZulu-Natal, Durban 4041, South Africa; ojok@ukzn.ac.za (K.E.O.); viranjay@ieee.org (V.M.S.)
[2] Department of Electronics Engineering, Birmingham City University, Birmingham B4 7XG, UK
* Correspondence: saha@ukzn.ac.za
† Presented at the 34th Southern African Universities Power Engineering Conference (SAUPEC 2026), Durban, South Africa, 30 June–1 July 2026.

Abstract

In this work, a multi-objective quantum particle swarm optimization (QPSO) algorithm is proposed to address the optimal scheduling of non-dispatchable sources in a microgrid energy management system (MGEMS) for residential areas under utility-induced demand-side management (DSM) programs. While taking economic and environmental aspects into account, the goal is to maximize energy management by integrating a variety of distributed generation (DG) units with an energy storage device. Using real-time meteorological data, two case studies were analyzed and simulated using MATLAB/Simulink R2025b. The simulation results reveal that the optimum optimization outcome among the case studies is obtained at a higher DSM load participation level of 10%. Without the involvement of DSM, MG's producing units in the first case had the highest carbon emissions of 797.110 kg and an overall operating cost of 267.10 €. Similarly, with the involvement of DSM, the second case had the lowest overall operating cost of 155.01 € and the lowest carbon emissions of 748.731 kg. The second case, which has optimal DG scheduling, is the suggested way to improve microgrid efficiency and provide a dependable power supply with low operating costs and emission reduction.

Keywords: demand-side management; distributed generation; microgrid; quantum particle swarm optimization

1. Introduction

Microgrid (MG) integration is a key implementation pathway in the decentralization of electrical networks, which has become a promising strategy in the quest for sustainable energy generation [1]. The process of creating an ideal operation strategy for the production plan in order to accomplish the optimal MG operation aim through the adjustment and control of controllable variables under complicated restrictions is known as the microgrid energy management system (MGEMS) problem [2,3]. MGs have attracted a lot of attention in electrical system networks due to their versatility and efficiency in integrating different renewable energy sources (RESs) to meet local energy demands. MGs may adapt to shifting energy demands while reducing their dependency on traditional fossil fuels by integrating a variety of dispersed energy sources, including solar PV, wind turbines, and energy storage devices [4]. Additionally, MGs reduce carbon gas emissions, improve voltage stability, increase energy supply reliability, and simplify demand responsiveness. The high unpredictability and variability of RESs, supply and demand matching, and microgrid

Academic Editor: Remy Tiako

Published: 5 June 2026

scalability are some of the disadvantages of MGs despite their many benefits. These challenges have led to focused research on microgrid energy management systems [5]. EMS is essential to increasing the reliability and efficiency of an MG system. Energy costs are reduced, leakage and consumption are reduced, and overall efficiency is increased when an effective EMS ensures the effective management of energy production, use, and storage. The energy management of MG's islanded and grid-connected modes varies according to operational requirements [6,7].

In MGEMS, energy scheduling has emerged as a crucial field of study due to the growing use of probabilistically regulated loads and naturally intermittent RESs. Researchers have analyzed a variety of optimization techniques to accomplish effective operational scheduling across a range of objectives and loading circumstances. In contrast to traditional optimization techniques, mixed integer linear programming (MILP) can yield optimal results under some conditions, but it is computationally demanding and has trouble handling the uncertainty that comes with RESs. The computational complexity of dynamic programming (DP), which is ideal for sequential decision-making, is severely limited by exponential complexity. Heuristic methods work well for traversing vast search spaces, but they frequently have drawbacks, including early convergence to local optima, being time-consuming, and being inefficient due to their high computational cost. Likewise, simple, rule-based approaches are not flexible enough to adjust to complex systems [8,9]. In this work, a multi-objective quantum particle swarm optimization (QPSO) methodology is presented to tackle the optimal scheduling challenges of non-dispatchable sources in MGEMS for residential areas under utility-induced DSM programs. Its quantum-inspired algorithms are especially well-suited for multi-objective optimization because they balance exploration and exploitation while enabling the effective exploration of intricate solution spaces. By combining swarm intelligence and quantum mechanical concepts, QPSO allows for a more thorough solution space search and effective multi-objective optimization. Its dynamic swarm behavior and quantum-inspired operators help it overcome the common problems of classical algorithms, such as managing complex, multi-modal, and non-linear objective functions [10]. By utilizing special qualities, such as quick convergence, resistance to local optima, and better management of multi-objective functions, which are frequently observed in conventional approaches, this clever strategy avoids premature convergence and stagnation [11].

Several recent studies have focused on using both deterministic and non-deterministic optimization strategies to solve the optimal energy scheduling issues in MGEMS. In [12], a stochastic framework was developed to achieve the optimal operational scheduling of hybrid AC–DC microgrids with integrated RESs and energy storage systems. The proposed approach employed an unscented transform-based stochastic load flow method to model uncertainties associated with load demand, market prices, and renewable generation (wind and solar PV). To enhance the search capability and avoid premature convergence, a two-stage improved modified crow search algorithm (CSA) was utilized. The framework was validated on a standard IEEE test system, confirming its feasibility and effectiveness. In Ref. [13], the authors proposed a modified shuffled frog leaping algorithm (MSFLA)-based optimization framework for the best day-ahead scheduling of an MG that contained various DG units and PEV kinds. The goal was to reduce the microgrid's running expenses. Additionally, three case studies were simulated, and the outcomes confirmed that this algorithm performed better than previous optimization techniques. In Ref. [14], the authors proposed an intelligent golden jackal optimization (GJO) algorithm for microgrid energy management in systems with battery storage and hybrid energy sources is presented in the manuscript. Power balance, generation restrictions, load demand, and energy storage charging/discharging dynamics are some of the major operational constraints that the model seeks to satisfy while minimizing operating costs. The suggested approach is tested against current optimization methods using MATLAB. According to simulation studies, the GJO strategy outperforms particle swarm optimization (PSO), artificial bee colony (ABC), and tabu search (TS) techniques in terms of efficiency of 96% and operational expenses around 2×10^6 \$.

In realistic MGEMS applications, the presence of weather-induced uncertainties renders deterministic models insufficient for effective dispatch of DG resources. The microgrid energy management system problem, which aims to achieve optimal energy scheduling while reducing operational costs and mitigating carbon emissions in the carbon trading market, is formulated in this work using a novel non-deterministic probabilistic technique of QPSO. The method actively modifies patterns of energy use and permits the effective control of non-critical loads by incorporating demand-side management algorithms into MGEMS. The work also looks into how residential load involvement in DSM affects utility power trading rates and microgrid operating costs.

2. Mathematical Formulation

The multi-objective function presented in this work considers both the MG minimum operating cost and the minimum optimization target for carbon emissions under the carbon trading market linked to the MG system.

$$Min f_1(\chi) = \sum_{t=1}^{T} \left\{ \begin{array}{c} \sum_{i=1}^{N_{DG}} u^i(t) P_{DG}^i(t) B_{DG}^i(t) + S_{DG}^i\left(u^i(t) - u^i(t-1)\right) + \\ \sum_{j=1}^{N_{BESS}} \left[u^j(t) P_{BESS}^j(t) B_{BESS}^j(t) + S_{BESS}^j\left(u^j(t) - u^j(t-1)\right) \right] \\ + P_{grid}^t(t) B_{grid}^t(t) \end{array} \right\} \tag{1}$$

$$Min f_2(\chi) = \sum_{t=1}^{T} \left(\begin{array}{c} \sum_{p}^{N_{MT}} C_{carbon}(t) \left(m_{carbon}^p(t) - C_{quota}(t) \right) + \\ \sum_{q}^{N_{FC}} C_{carbon}(t) \left(m_{carbon}^q(t) - C_{quota}(t) \right) \end{array} \right) \tag{2}$$

Equations (1) and (2) ensure that the MG scheduling strategy not only minimizes operational cost but also reduces environmental impact under a carbon trading market. $f_1(\chi)$ represents the operational cost, which encompasses the cost of running each DG unit as well as the power interaction between the utility and the MG. $f_2(\chi)$ quantifies the total carbon trading cost over the scheduling horizon T. The variables N_{DG} and N_{BESS} represent the overall number of DG and BESS units connected to the MG network. The bid costs of DG units, BESS units, and the utility at the hours of time 't' are denoted as $B_{DG}^i(t)$, $B_{BESS}^k(t)$, and $B_{grid}^t(t)$. While $P_{DG}^i(t)$, $P_{BESS}^j(t)$, and $P_{grid}^t(t)$ are the exchanged active electricity pricing for the utility, BESS, and DG sources, $C_{carbon}(t)$ is the carbon trading market's current price, $m_{carbon}^p(t)$, and $m_{carbon}^q(t)$ are the MGs carbon emissions from the MT and FC, and $C_{quota}(t)$ is the quantity of carbon allowances decided by the loads [15,16]. In this work, managing an MG for optimal operation requires solving the constraints optimization problem.

2.1. Power Balance Constraints

The power balance constraint is one of the key limitations for MGEMS's energy scheduling to function consistently. It requires that the active power generated by the utility, BESS, and DG sources match the system load demand.

$$\sum_{t=1}^{T} P_{load}(t) = \sum_{t=1}^{T} \left(\begin{array}{c} \sum_{i=1}^{N_{DG}} P_{DG}^i(t) + \sum_{j=1}^{N_{BESS}} P_{BESS}^j(t) \\ + P_{grid}^t(t) \end{array} \right) \tag{3}$$

2.2. Active Power Generation Constraint

The active power output of each DG unit and the power transmitted between the utility and the MG are restricted to predetermined minimum and maximum values to guarantee system security and stability.

$$\left.\begin{array}{c} P^{i}_{DG,min} \leq P^{i}_{DG}(t) \leq P^{i}_{DG,max} \\ P^{j}_{BESS,min} \leq P^{j}_{BESS}(t) \leq P^{j}_{BESS,max} \\ P^{t}_{grid,min} \leq P^{t}_{grid} \leq P^{t}_{grid,max} \end{array}\right\} \quad (4)$$

$P^{i}_{DG,min}$ and $P^{i}_{DG,max}$, $P^{k}_{BESS,min}$ and $P^{k}_{BESS,max}$, and $P^{t}_{grid,min}$ and $P^{t}_{grid,max}$ represent the minimum and maximum active power outputs for each scheduling period in MGEMS. Additionally, the control variables are self-constrained, but the dependent variable must be added as a quadratic penalty term in the objective function. This term increases the objective function by a penalty factor termed 'λ_{pen}', which is the square of the difference between the actual and limiting values of the dependent variable. Any unworkable solution discovered during the optimization process is ignored [17,18].

$$MinF(\chi) = \sum_{t=1}^{T} TC^{t} + \lambda_{pen}\left(P^{t}_{grid} - P^{t}_{grid,lim}\right)^{2} \quad (5)$$

2.3. Demand-Side Flexibility Constraint

DSM in a microgrid increases operating efficiency, lowers costs, lowers carbon emissions, and improves consistency. DSM reduces electricity bills for customers and optimizes system costs for operators [19]. Equation (6) enforces a demand-side response mechanism by ensuring that storage discharge, rather than external supply, satisfies a minimum percentage of demand. The response and storage weighting coefficients show the flexibility of demand shifting and storage usage. Before using grid electricity, the limitation ensures that distributed resources are effectively utilized.

$$Min\ F = \sum_{t=1}^{T}\left(\varphi_{t}^{dem} * \tau_{t}^{response} - \zeta_{t}^{BESS,dis} * \tau_{t}^{storage}\right) \geq \theta^{demand,shifting} \quad (6)$$

3. Modeling of DG Units

In this work, a typical low-voltage grid-connected MG model, as shown in Figure 1, is considered for assessing the proposed QPSO architecture. The model consists of the MG central controller (MGCC), which is in charge of monitoring and controlling the power exchange between the utility and the MG. The primary duty of MGCC is to provide local controllers with power references to meet power balance requirements for the designated time T. The load controller (LC) and micro-source controller (MC), which are in charge of delivering or absorbing excess (deficit) energy to satisfy power requirements, assist this endeavor. The architecture includes a number of distributed generation (DG) units, such as fuel cells (FC), wind turbines (WT), gas-fueled microturbines (MT), and solar photovoltaic (PV) systems, in addition to an energy storage device. All DG sources are thought to produce active power with a power factor of unity. In addition, the MGCC's actions establish a power exchange link between the utility and the MG to exchange energy throughout the day. The total energy demand of the MG's system adds up to 1695 kWh. The unit time interval is 1 h, and the dispatching time is one day (24 h).

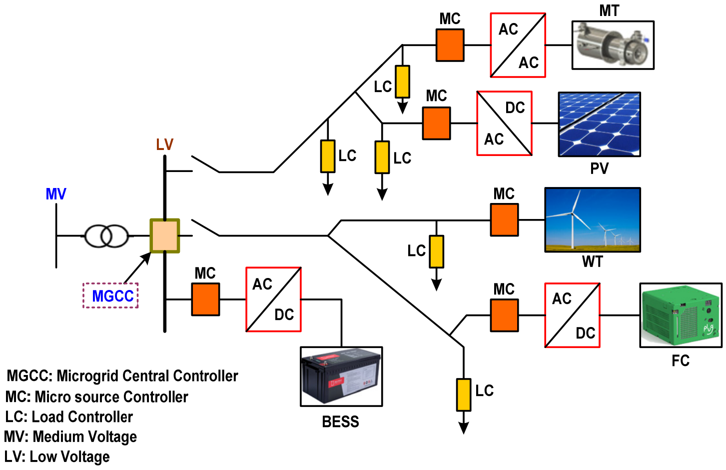

Figure 1. A model of the low-voltage connected MG.

3.1. Solar PV Model

The PV system's power output may be impacted by the module features and meteorological parameters, such as solar irradiation of I_s and the ambient temperature of T_a. The estimated power output P_{PV} from the PV module is as follows [20]:

$$P_{PV} = P_{STC} \frac{I_s}{1000} * (1 + \alpha(T_c - 25)) \tag{7}$$

$$T_c = T_a + \frac{I_s}{800} * (T_{NOCT} - 20) \tag{8}$$

where P_{STC} represents the maximum power (W) of the solar module under standard test conditions (STC). On the surface of the photovoltaic module, I_s represents the sun's irradiation $(\mathrm{W/m^2})$. T_c denotes the temperature of the photovoltaic cell (module) $(^\circ\mathrm{C})$ and α represents the temperature coefficient for power $\left(^\circ\mathrm{C}^{-1}\right)$. T_a represents the ambient temperature $(^\circ\mathrm{C})$, and T_{NOCT} represents the normal operating cell temperature $(^\circ\mathrm{C})$ of the module.

3.2. Wind Turbine Model

The main factor influencing a wind turbine's power output is the wind's sporadic nature. To calculate a wind turbine's power output, two important factors must be considered: the wind speed at a particular place and the wind turbine's power curve. A function with three (3) separate parts can be used to depict the power curve of a wind turbine [20]:

$$P_{WT} = \begin{cases} 0 & v \le v_{ci} \\ \dfrac{v^2 - v_{ci}^2}{v_{nom}^2 - v_{ci}^2} * P_{WT,nom} & v_{ci} < v \le v_{nom} \\ P_{nom} & v_{nom} < v \le v_{co} \end{cases} \tag{9}$$

where $P_{WT,nom}$, v_{nom}, v_{ci}, and v_{co} are nominal power, nominal wind speed, cut-in wind speed, and cut-out wind speed, respectively, P_{WT} is the power output of the wind turbine (kW), and v is the wind speed $(\mathrm{m/s})$.

3.3. Calculation Cost of DG Units

The cost function estimates of DG units are estimated by the authors in Ref. [21]. The following is how the DG bids are stated, and similarly, MT and FC bids are determined as follows:

$$B_{DG} = C_{fuel} * \frac{P_{DG}}{\eta_{DG}} + C_{inv} \tag{10}$$

$$C_{inv}= DC * \frac{P_{DGnom}}{PC} \tag{11}$$

$$DC= \frac{r(1+r)^n}{(1+r)^n - 1} * IC \tag{12}$$

where B_{DG} denotes the total operating cost of the DG, C_{fuel} represents the fuel cost coefficient or cost of the fuel per unit energy, P_{DG} is the output power generated by the DG, η_{DG} is the efficiency of the DG, C_{inv} is the annual investment cost of the DG, P_{DGnom} denotes the nominal power rating of the DG, PC is the payback period/capacity parameter, DC is the total capital cost of DG, r represents the interest rate, n denotes the life span of the DG units, and IC represents the cost of installing DG units.

3.4. Optimization Approach

This section explains the suggested optimization that achieves the best MG performance while adhering to overall operational cost and environmental limitations. QPSO is one of the most popular optimization techniques that draws inspiration from quantum physics. Quantum mechanics-inspired optimization provides a fundamental change in problem-solving strategies when compared to conventional heuristics, meta-heuristics, and other optimization techniques. Quantum physics concepts and the collective intelligence of particle swarm optimization (PSO) are combined in QPSO [22]. At each iteration, the particle's position is updated in accordance with Equations (13) and (14).

$$x_{p,q}(t+1)= P_{p,q}(t) \pm \xi * \left|mbest_{p,q}(t) - x_{p,q}(t)\right| * In\left(\frac{1}{u}\right) \tag{13}$$

$$P_{p,q}(t)= \left(\varphi * P_{p,q}(t) + (1-\varphi)G_q(t)\right) \tag{14}$$

$$\varphi= \frac{c_1 r_1}{c_1 r_1 + c_2 r_2} \tag{15}$$

$$L_{p,q}(t)= 2\xi\left|C_q(t) - X_{p,q}(t)\right| \tag{16}$$

$$C_q(t)= \frac{1}{M}\sum_{p=1}^{M} P_{p,q}(t) \tag{17}$$

Provided that $(1 \leq p \leq N)$ and $(1 \leq q \leq M)$, in M iterations, every particle with a dimension of 'D' converges to its local attractor $P = P_1, P_2, P_3, \ldots, P_D$. The acceleration coefficients are c_1 and c_2, the randomly distributed, regularly distributed integers within [0, 1] are r_1, r_2 and u, and the average best position of the particle swarm is represented as $C_q(t)$. The personal best and global best positions of the p^{th} particle in the q^{th} iteration are indicated by $P_{p,q}$ and G_q, respectively. $L_{p,q}(t)$ is the length of the particle's q^{th} dimensional potential well following the p^{th} iteration, which can limit the particle's spatial search range. For every iteration, the mean of the personal best locations $mbest_{p,q}(t)$ is needed to update the lagged particles in the population. The contraction–expansion coefficient, or parameter ξ, is defined as $\xi = 1 - (1.0 - 0.5) * \mathrm{k/Gm}$ in the context of quantum mechanics. Thus, the variable k represents the current iteration count.

$$mbest_{p,q}(t) = \left(\frac{1}{N}\sum_{p=0}^{N} P_{p,1}(t), \frac{1}{N}\sum_{p=0}^{N} P_{p,2}(t) \ldots, \frac{1}{N}\sum_{p=0}^{N} P_{p,D}(t)\right) \tag{18}$$

In this work, the generalized QPSO framework for energy scheduling of the MGEMS problem, subject to utility-induced DSM and without DSM level of participation, is presented. The proposed flowchart of the multi-objective QPSO algorithm is shown in Figure 2.

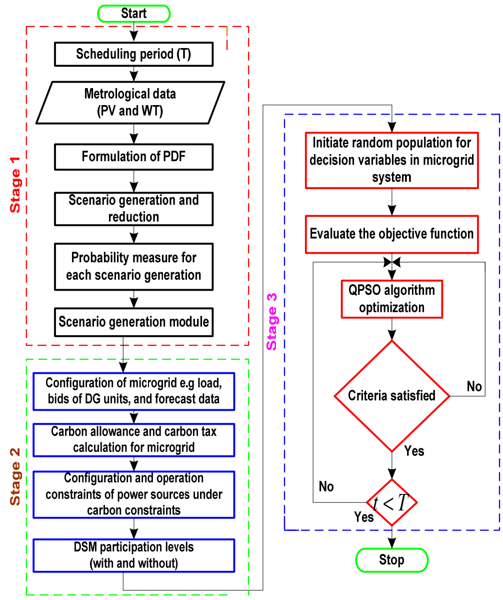

Figure 2. The flowchart of the QPSO algorithm.

3.5. Implementation of the Proposed Optimization

This section examines how the proposed optimization is implemented to optimize energy scheduling and examines how the demand of load participation affects a typical microgrid. This scenario has been studied using the standard MG, which includes BESS, FC, WT, PV, and MT. Power exchange is made possible when necessary via the point of common connection (PCC), which connects the MG to the utility grid. In order to capture conditions of increased demand and decreased renewable generation, the collection consists of real-time meteorological data collected during the winter. All of the power sources in the MG have their maximum and minimum power outputs listed in Table 1. The simulation parameters of the proposed optimization are listed in Table 2.

Table 1. DG units output power capacity.

Unit	Type	Min Power (kW)	Max Power (kW)
1	MT	6	30
2	FC	3	30
3	PV	0	25
4	WT	0	15
5	BESS	−30	30
6	Utility	−30	30

Table 2. Simulation parameters.

Variables	Values
Max number of iterations ($iter_{max}$)	50–200
Acceleration coefficients (c_1, c_2)	2
Contraction–expansion coefficient (ξ)	0.5
Randomly distributed integers	0, 1
Percentage of load participation	10%
Current iteration count (k)	0.5

4. Result and Discussion

In this work, two (2) case studies are taken into consideration. Case 1, which is regarded as the base case, uses a QPSO optimizer to solve the MG scheduling problem to minimize overall operating costs and reduce carbon emissions. The base case analyzes the operating cost effects of utility and DG units' power exchange in the absence of the demand-side load participation. The economic power dispatch of DG sources without demand-side load participation using the QPSO optimizer is shown in Figure 3. Because their bids are lower than those of the other units during the investigated period, the FC and the utility supply a major portion of the load during the 1 h to 8 h and 23 h to 24 h periods. As market prices rise between 9 h and 17 h and 21 h and 22 h, more MT is produced, and excess energy is exported from the MG to the utility. In order to improve MG resilience for each DG source, the dispatch solution prioritizes BESS utilization during the time of high energy prices, which is from 9 h to 17 h, and minimizes MG–utility power exchange between 18 h and 20 h. Furthermore, the output characteristics of WT and PV differ, which contribute to the MG during peak demand from 9 h to 16 h, increasing energy exports to the utility. The scheduling running cost of MG's generating units comes to 267.10 €. In case 2, the economic power dispatch of DG sources with a demand-side load participation level of 10% involved, using the QPSO optimizer, is shown in Figure 4. The simulation's outcome clearly shows that, in comparison to case 1, the overall operating cost decreased. Similarly, the output power of MT reaches its greatest during periods of high market prices and its minimum during periods of low market prices, but the output power of FC reaches its maximum value throughout the day. During periods of low utility market rates, the BESS is set to charge between 5 h and 7 h and between 23 h and 24 h. During peak hours, the battery uses its stored energy to power the load and exports the remaining energy to the grid. Because of the increased penetration of FC, it is seen that the power output of MT decreases. The power output regulations governing the WT and PV RESs are different. During peak demand, which occurs between 9 h and 14 h, it is noticed that PV and WT contribute to MG, increasing the amount of energy exported to the utility. Thus, the scheduling running cost of MG's generating units steadily falls to 155.01 €. The percentage decrease in MG operation costs is 41.97% as compared to case 1, which does not take DSM participation into account.

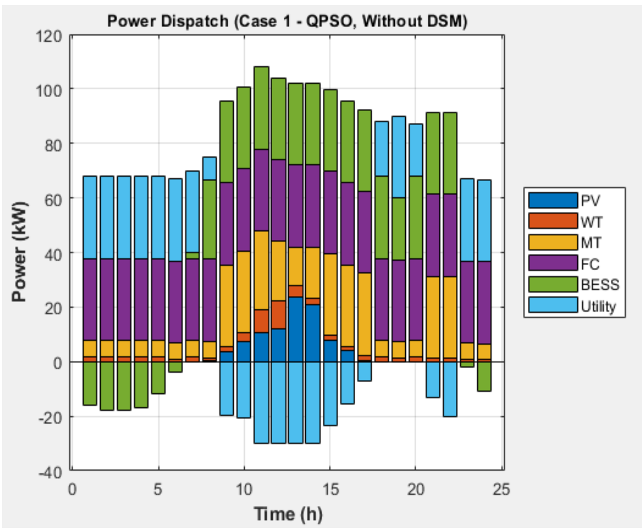

Figure 3. The power dispatch of DG without DSM.

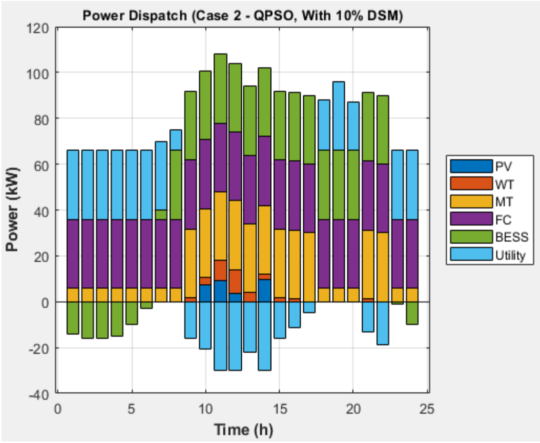

Figure 4. The power dispatch of DG with 10% DSM.

Consequently, the optimal scheduling results for emission dispatch under case 1 carbon trading are shown in Figure 5. Since the only traditional power sources in the proposed MG that use natural gas or biogas are microturbines (MT) and fuel cells (FC). When compared to other DG units, these emit a lot more carbon dioxide (CO_2) per kilowatt of generation. At 1 h, 3 h, 7 h, and 9 h, respectively, the MT output is higher. The MT's power production will be raised to charge the BESS during the 2 h, 6 h, and 14 h periods, which correspond to the off-peak demand period, regarding the carbon trading market. Likewise, this reasoning holds true for fuel cells as well. The hours of 16 h, 23 h, and 24 h are regarded as peak demand. By increasing MT's power output, the cost of electricity purchased drops between 9 h and 15 h. The QPSO can reduce carbon emissions to 797.110 kg once the carbon trading market is implemented. Similarly, the optimal scheduling results for each power source under case 2 carbon emission are shown in Figure 6. At 1 h, 6 h, 7 h, and 10 h, respectively, the MT output is higher. In terms of the carbon trading market, the MT's power output will be increased to charge the BESS throughout the 2 h and 3 h periods, which correspond to the off-peak demand period. The hours of 12 h, 14 h, and 23 h are regarded as peak demand. By increasing MT's power output, the cost of electricity purchased drops during the period of 22 h. The QPSO can reduce carbon emissions to 748.731 kg. Table 3, presents the performance metrics results. The performance evaluation shown in Figure 7 indicates that the MG operational cost and carbon emission dramatically decrease with the integration of the DSM load participation level.

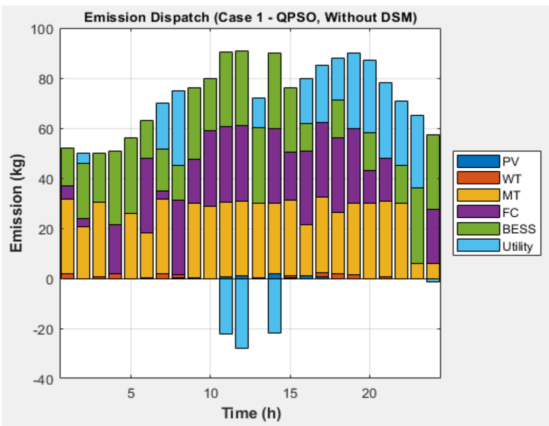

Figure 5. The emission dispatch without DSM.

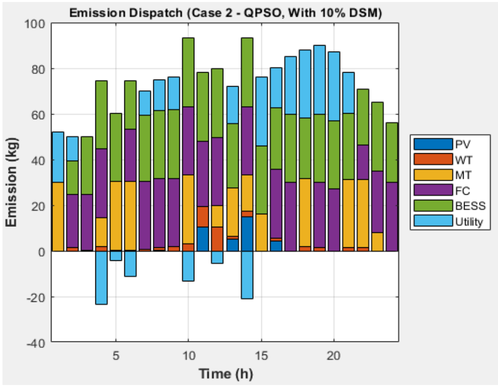

Figure 6. The emission dispatch with 10% DSM.

Table 3. Simulation results.

Case ID	Total Operating Cost (€)	Carbon Emission (kg)
Case 1	267.10	797.110
Case 2	155.01	748.731

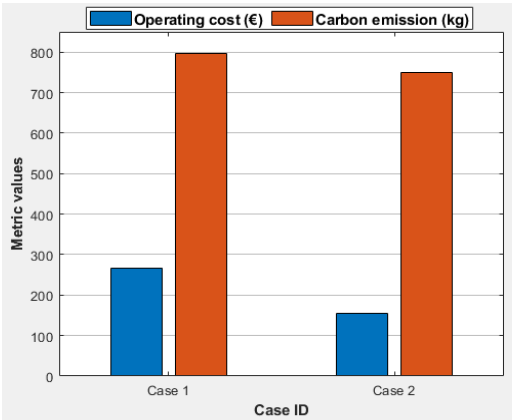

Figure 7. The performance of the scheduling profile of the MG operation.

5. Conclusions

In grid-connected MG, the increasing integration of RESs has made it more difficult to achieve the best possible economic and emission-efficient power dispatch in the face of uncertainty. Therefore, this work designs a multi-objective optimization framework to handle the scheduling in MGEMS problems under utility-induced DSM programs. In this work, a three-stage scenario architecture is proposed. Two case studies were examined using real-time meteorological data. A total load participation level 10% is used to assess the effect of demand-side load participation in MG operation. The obtained result justified that the MG operational cost and carbon emission dramatically decrease with the integration of the DSM load participation level. The findings of this work demonstrate that the QPSO approach is effective in solving the MGEMS problem and providing techno-economic advantages to utility and MG operators.

Author Contributions: Conceptualization, K.E.O., A.K.S., and V.M.S.; methodology, K.E.O., A.K.S., and V.M.S.; software, K.E.O.; validation, K.E.O., A.K.S., and V.M.S.; formal analysis, K.E.O.; investigation, K.E.O.; resources, K.E.O.; data curation, K.E.O.; writing—original draft preparation, K.E.O.; writing—review and editing, A.K.S. and V.M.S.; visualization, A.K.S. and V.M.S.; supervision, A.K.S. and V.M.S.; project administration, A.K.S. and V.M.S. All authors have read and agreed to the published version of the manuscript.

Funding: This research received no external funding.

Institutional Review Board Statement: Not applicable.

Informed Consent Statement: Not applicable.

Data Availability Statement: Data is already embedded in the article.

Conflicts of Interest: The authors declare no conflicts of interest.

References

1. Hematian, H.; Askari, M.T.; Ahmadi, M.A.; Sameemoqadam, M.; Nik, M.B. Robust Optimization for Microgrid Management with Compensator, EV, Storage, Demand Response, and Renewable Integration. *IEEE Access* **2024**, *12*, 73413–73425. [CrossRef]
2. Tekisi, T.; Srivastava, V.M. Analytical Approach towards Low-Power Device (Differential Amplifier) Using DG MOSFET. In Proceedings of the 31st South African Universities Power Engineering Conference (SAUPEC), Johannesburg, South Africa, 24–26 January 2023; pp. 152–156.
3. Saeed, M.H.; Fangzong, W.; Kalwar, B.A.; Iqbal, S. A Review on Microgrids: Challenges and Perspectives. *IEEE Access* **2021**, *9*, 166502–166517. [CrossRef]
4. Marino, C.A.; Marufuzzaman, M. A Microgrid Energy Management System Based on Chance-Constrained Stochastic Optimization and Big Data Analytics. *Comput. Ind. Eng.* **2020**, *143*, 106392. [CrossRef]
5. Ojo, K.E.; Saha, A.K.; Srivastava, V.M. Microgrids' Control Strategies and Real-Time Monitoring Systems: A Comprehensive Review. *Energies* **2025**, *18*, 3576. [CrossRef]
6. Imran, A. Heuristic-Based Programmable Controller for Efficient Energy Management under Renewable Energy Sources and Energy Storage System in Smart Grid. *IEEE Access* **2020**, *8*, 139587–139608. [CrossRef]
7. Ojo, K.E.; Saha, A.K.; Srivastava, V.M. A Critical Review of Advanced Protection Devices in AC Microgrid. *IEEE Access* **2025**, *13*, 203931–203971. [CrossRef]
8. Shirley, J.A.J.; Pooja, R.P.; Reddy, M.J.B. Metaheuristic Algorithm-Based Energy Management System for Electric Vehicle Charging Station. *IEEE Access* **2024**, *12*, 116354–116367. [CrossRef]
9. Aviles, D.A.; Pascual, J.; Guinjoan, F.; Gutierrez, G.G.; Orguera, R.G.; Proano, J.L.; Sanchis, P.; Motoasca, T.E. An Energy Management System Design Using Fuzzy Logic Control: Smoothing the Grid Power Profile of a Residential Electro-Thermal Microgrid. *IEEE Access* **2021**, *9*, 25172–25188. [CrossRef]
10. Shaterabadi, M.; Jirdehi, M.A. Multi-Objective Stochastic Programming Energy Management for Integrated INVELOX Turbines in Microgrids: A New Type of Turbines. *Renew. Energy* **2020**, *145*, 2754–2769. [CrossRef]
11. Goh, H.H.; Shi, S.; Liang, X.; Zhang, D.; Dai, W.; Liu, H.; Wong, S.Y.; Kurniawan, T.A.; Goh, K.C.; Cham, C.L. Optimal Energy Scheduling of Grid-Connected Microgrids with Demand Side Response Considering Uncertainty. *Appl. Energy* **2022**, *327*, 120094. [CrossRef]
12. Papari, B.; Edrington, C.S.; Bhattacharya, I.; Radman, G. Effective Energy Management of Hybrid AC–DC Microgrids with Storage Devices. *IEEE Trans. Smart Grid* **2019**, *10*, 193–203. [CrossRef]
13. Zeng, X.; Nazir, M.S.; Khaksar, M.; Nishihara, K.; Tao, H. A Day-Ahead Economic Scheduling of Microgrids Equipped with Plug-In Hybrid Electric Vehicles Using Modified Shuffled Frog Leaping Algorithm. *J. Energy Storage* **2021**, *33*, 102021. [CrossRef]
14. Kumar, R.P.; Karthikeyan, G. A multi-objective optimization solution for distributed generation energy management in microgrids with hybrid energy sources and battery storage system. *J. Energy Storage* **2024**, *75*, 109702. [CrossRef]
15. Moghaddam, A.A.; Seifi, A.; Niknam, T.; Pahlavani, M.R.A. Multi-Objective Operation Management of a Renewable MG (Microgrid) with Back-Up Micro-Turbine/Fuel Cell/Battery Hybrid Power Source. *Energy* **2011**, *36*, 6490–6507. [CrossRef]
16. Liu, H.; Du, W.; Guo, Z. A Multi-Population Evolutionary Algorithm with Single Objective Guide for Many-Objective Optimization. *Inf. Sci.* **2019**, *503*, 39–60. [CrossRef]
17. Awelewa, A.; Ezenwanne, E.; Ojo, K.; Samuel, I.; Olawale, P. Impact of a Web-Based Crowdfunding Application for Renewable Energy Projects in Nigeria. In Proceedings of the International Conference on Smart Applications, Communications and Networks (SmartNets), Istanbul, Turkey, 25–27 July 2023; pp. 1–8.
18. Khan, Z.A.; Jayaweera, D. Smart Meter Data-Based Load Forecasting and Demand Side Management in Distribution Networks with Embedded PV Systems. *IEEE Access* **2020**, *8*, 2631–2644. [CrossRef]
19. Paul, K.; Jyothi, B.; Kumar, R.S.; Singh, A.R.; Bajaj, M.; Kumar, B.H.; Zaitsev, I. Optimizing Sustainable Energy Management in Grid-Connected Microgrids Using Quantum Particle Swarm Optimization for Cost and Emission Reduction. *Sci. Rep.* **2025**, *15*, 5843. [CrossRef] [PubMed]

20. Kumar, R.S.; Raghav, L.P.; Raju, D.K.; Singh, A.R. Intelligent Demand Side Management for Optimal Energy Scheduling of Grid-Connected Microgrids. *Appl. Energy* **2021**, *285*, 116435. [CrossRef]
21. Radosavljević, J.; Milovanović, M.; Arsić, N.; Jovanović, A.; Perović, B.; Vukašinović, J. Optimal Power Dispatch in Distribution Networks with PV Generation and Battery Storage. In Proceedings of the 9th International Conference on Electrical, Electronic and Computing Engineering (IcETRAN), Novi Pazar, Serbia, 6–9 June 2022; pp. 6–9.
22. Xi, M.; Wu, X.; Sheng, X.; Sun, J.; Xu, W. Improved Quantum-Behaved Particle Swarm Optimization with Local Search Strategy. *J. Algorithms Comput. Technol.* **2016**, *11*, 3–12. [CrossRef]